

# Electronic Origin of Linearly Polarized Emission in CdSe/CdS Dot-in-Rod Heterostructures

Josep Planelles,\* Fernando Rajadell, and Juan I. Climente

*Departament de Química Física i Analítica, Universitat Jaume I, E-12080, Castelló de la Plana,  
Spain*

E-mail: josep.planelles@uji.es

---

\*To whom correspondence should be addressed

## **Abstract**

Seeded CdSe/CdS nanorods exhibit intense polarized emission along the rod main axis. The degree of linear polarization cannot be explained by dielectric effects alone, an additional electronic contribution is present whose nature has not been settled up to date. Using multi-band k-p theory, we analyze the potential influence of several factors affecting excitonic emission and show that shear strain is the main electronic mechanism promoting linear polarization. It favors energetically light hole excitons over heavy hole ones, via deformation potential, and makes their radiative recombination faster via piezoelectricity. Implications of this mechanism are that linear emission can be enhanced by growing long but thin CdS shells around large, prolate CdSe cores, which indeed supports and rationalizes recent experimental findings. Together with the well-known dielectric effects, these results pave the way for controlled degree of linear polarization in dot-in-rods through dedicated structural design.

The optoelectronic properties of semiconductor colloidal nanocrystals can be widely tuned by tailoring their size, shape and composition, which makes them competitive building blocks for existing and emerging technologies alike.<sup>1</sup> One of the most promising types of nanocrystals for room temperature optical applications in the visible spectrum are heterostructured CdSe/CdS dot-in-rods (DiRs), where a rod-shaped CdS shell is grown around a nearly spherical CdSe core.<sup>2</sup> Added to a well established synthetic route,<sup>3-5</sup> CdSe/CdS DiRs exhibit narrow emission line width,<sup>6</sup> high quantum yield,<sup>3-5</sup> optical gain,<sup>7,8</sup> tunable Stokes shifts,<sup>3</sup> tunable exciton lifetime<sup>9</sup> and large two-photon absorption cross section.<sup>10</sup>

As compared to other CdSe/CdS nanocrystals, like giant-shell quantum dots,<sup>11</sup> DiRs present the additional advantage of displaying linearly polarized band edge absorption and emission.<sup>3-5</sup> The origin of such a linear polarization is however a controversial issue. It is widely accepted that there is a contribution arising from the dielectric mismatch between the inorganic structure and its surface ligands. Because of the anisotropic shape, dielectric screening of electromagnetic fields favors light absorption and emission along the long axis of the rod, similar to the case of CdSe nanorods.<sup>12,13</sup> But the dielectric effect predicts the degree of linear polarization increase monotonically with the aspect ratio of the nanocrystal, saturating for aspect ratios above  $\sim 10$ . This is in contradiction with a number of experiments, which have reported non-monotonic dependence on the aspect ratio<sup>15</sup> and polarization degrees well beyond the limit of the dielectric model.<sup>16-18</sup> An additional source of optical anisotropy must be present, presumably related to electronic degrees of freedom. By analogy with CdSe nanorods,<sup>14</sup> it has been postulated that the top of the valence band in DiRs is formed by light holes (LH) instead of heavy holes (HH), as the former promote emission along the  $c$ -axis of wurtzite nanocrystals, which is aligned with the rod long axis. Why this occurs is still unclear, because band edge exciton recombination in DiRs takes place inside the core, that is nearly spherical. One would then expect the ground state to be HH. In fact, although wurtzite CdSe seeds are slightly prolate, they do not show steady state optical anisotropy by themselves.<sup>16</sup> Encapsulation within an anisotropic CdS shell seems to be a requisite to that end.

Recent experiments have attempted to elucidate the role of different morphological and struc-

tural parameters in determining the degree of linear polarization.<sup>15–18</sup> Sitt *et al.* showed that elongated (rod shaped) cores strengthen linear polarization as compared to usual (nearly-spherical) ones.<sup>16,17</sup> Diroll *et al.* suggested that thin anisotropic shells around the core further favor linear polarization,<sup>18</sup> but Vezzoli *et al.* pointed out this could be simply due to the large size of the CdSe cores in such samples, as in their work large cores seem to promote LH ground states and hence linearly polarized emission.<sup>15</sup> However, other works present DiRs with equally large core sizes and yet they report HH ground states.<sup>19</sup> The precise shape of the core may make the difference.<sup>15</sup> All of these are phenomenological observations inferred from systematic experiments, which do not answer the fundamental question of what quantum-physical mechanism makes DiRs emit net linearly polarized light. Deeper theoretical understanding is needed to unravel the influence of the many competing factors. This is ultimately needed to design DiRs with deterministic control of the optical anisotropy. The goal of this work is then to clarify the origin of the electronic contribution to the linear polarization of CdSe/CdS DiRs, and how it relates to the structural parameters.

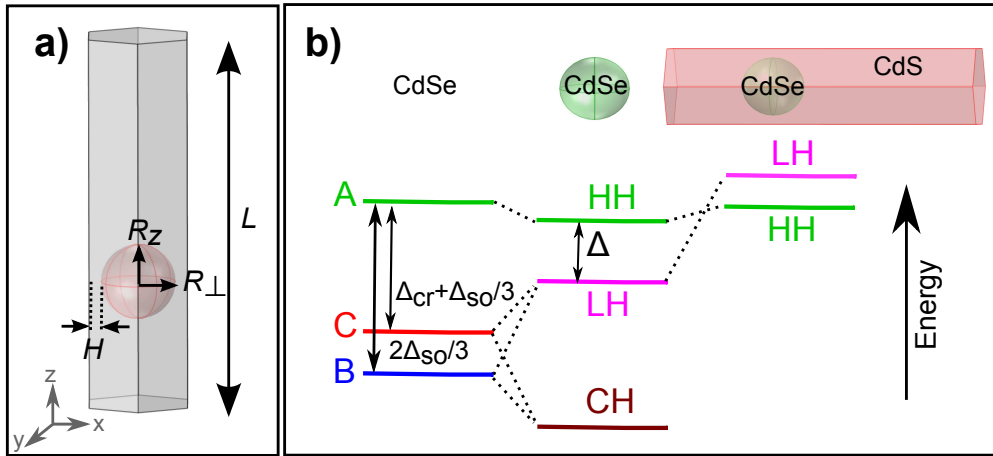


Figure 1: (a) Schematic of the DiR under study. (b) Evolution of valence subbands in different cases. Left: uncoupled wurtzite subbands. Center: subbands coupled by confinement and spin-orbit interaction. Right: subbands in a DiR with LH ground state.  $\Delta$  is the net splitting between HHs and LHs.

We consider DiRs like that in Fig.1(a), with an ellipsoidal CdSe core of radius  $R_z$  along the  $z$ -direction ( $c$ -axis) and  $R_\perp$  in the  $x, y$  directions. The core is at  $1/3$  of the CdS shell height, whose length is  $L$  and has its  $c$ -axis also aligned along  $z$ . The shell thickness between the core and the

lateral sides of the shell is denoted as  $H$ . Both CdSe and CdS have wurzite crystal structure. We then calculate valence band holes using a 6-band k·p Hamiltonian.<sup>20,21</sup> In this picture, the valence band splits into  $A$  subband (Bloch functions  $|P_+ \uparrow\rangle, |P_- \downarrow\rangle$ ),  $B$  subband ( $|P_+ \downarrow\rangle, |P_- \uparrow\rangle$ ) and  $C$  subband ( $|P_z \uparrow\rangle$  and  $|P_z \downarrow\rangle$ ).  $C$ -subband holes are responsible for the linearly polarized absorption and emission along the  $z$ -direction, because when recombining radiatively with electrons (Bloch functions  $|S \uparrow\rangle$  and  $|S \downarrow\rangle$ ), the dipole moment element  $\langle S \uparrow | \mu_z | P_X \uparrow \rangle$  is only finite if  $X = Z$ .

In CdSe,  $A$ ,  $B$  and  $C$  subbands are energetically sorted as shown on the left of Fig.1(b). The top of the valence band is formed by  $A$  holes, which are split from  $C$  and  $B$  holes by the crystal field splitting  $\Delta_{cr}$  and the split-off spin-orbit splitting  $\Delta_{so}$ . In a nearly-spherical CdSe quantum dot, confinement and spin-orbit interaction lead to some changes, as shown in the center of Fig.1(b).  $A$ -subband remains on top, its mixing with other subbands being small. By analogy with zinc-blende structures, it is often referred to as HH subband. By contrast,  $B$ - and  $C$ -subbands undergo severe coupling to form LH and split-off (CH) subbands. Notice that LHs inherit from  $C$  holes the capacity to emit linearly polarized light. We shall label  $\Delta$  the energy splitting between the top-most HH state (hole state with predominant HH character) and the top-most LH state (predominant LH character), i.e.  $\Delta = E_{HH} - E_{LH}$ . Upon growth of an anisotropic CdS shell around the dot, experiments suggest the ground state can change from HH to LH, as shown on the right of Fig.1(b). This means  $\Delta$  changes from positive to negative. We shall try to determine which physical mechanism and structural conditions make this possible. To this end, we decompose  $\Delta$  as:

$$\Delta = \Delta_{int} + \Delta_{shape} + \Delta_{strain} + \Delta_{coulomb}. \quad (1)$$

Here  $\Delta_{int}$  is the intrinsic splitting at  $k = 0$ , owing to spin-orbit interaction and the hexagonal lattice crystal field splitting. For CdSe,  $\Delta_{int} = 23.4$  meV, which implies the ground state in bulk is HH.<sup>20</sup>  $\Delta_{shape}$  is the shape splitting, which accounts for quantum confinement and spontaneous polarization. The latter introduces a small electric field along the  $c$ -axis,<sup>22</sup> whose influence we find to be minor. By contrast, quantum confinement can be important. The anisotropic masses of the valence

band stabilize HHs when confinement along the  $c$ -axis is comparable or stronger than the transversal one, and LHs otherwise.<sup>23</sup> Because wurtzite cores tend to deviate from sphericity and become slightly prolate along the  $c$ -axis, this could favor LHs. For cores with sufficiently large aspect ratio, it could even lead to a LH ground state.<sup>24</sup>  $\Delta_{strain}$  is the splitting induced by strain via deformation potential (DP) and piezoelectricity (PZ). Strain-induced DP is felt differently by HH and LHs.<sup>20</sup> Indeed, experiments with CdSe/CdS dot-in-plates reported unusually large and positive values of  $\Delta$ , which were interpreted using simple models to be a consequence of the anisotropic pressure exerted by the shell upon the core.<sup>27</sup> Because DiRs are the opposite case to dot-in-plates, with prolate shells instead of oblate ones, it has been speculated this could be a key mechanism leading to small or negative  $\Delta$ .<sup>15</sup> We will try to verify this point. Piezoelectricity, in turn, can stretch and separate electron and hole wave functions along the  $c$ -axis of CdSe/CdS heterocrystals,<sup>25,26</sup> which may also affect the HH-LH splitting.  $\Delta_{coulomb}$  represents the influence of excitonic Coulomb attraction. Since the electron in DiRs is partly delocalized over the shell,<sup>28,29</sup> it may as well stretch the hole wave function along the  $c$ -axis, hence stabilizing LHs.

We start by analyzing the influence of the shell dimensions on  $\Delta$ . We consider DiRs with a fixed spherical core of radius  $R = 1.5$  nm, shell length  $L = 50$  nm, and varying shell thickness  $H$ . As can be seen in Fig.2(a), the net HH-LH splitting rapidly decreases as the shell becomes thinner. This qualitatively supports the conclusion inferred from recent experiments, that thin shells enhance optical anisotropy.<sup>18</sup> Notice, however, that the experiments included an inverse correlation between shell thickness and core size, which made it difficult to disentangle the influence of the two factors. Since we have fixed core radius, our calculations allow us to confirm the role of  $H$  unambiguously. Notice also that in spite of the decrease,  $\Delta$  remains positive even for the thinnest shells. This suggests that thin shells alone cannot justify a LH ground state. Further factors are needed, which we will discuss below. Before that, it is useful analyzing why a thin shell reduces  $\Delta$ . To this end, in Fig.2(b) we plot the dependence of different terms of Eq. (??) on  $H$ .  $\Delta_{shape}$  is roughly constant except for very thin shells. This is because the hole is mainly confined inside the core and hence little sensitive to changes of the shell confinement potential.  $\Delta_{coulomb}$  is also quite insensitive to

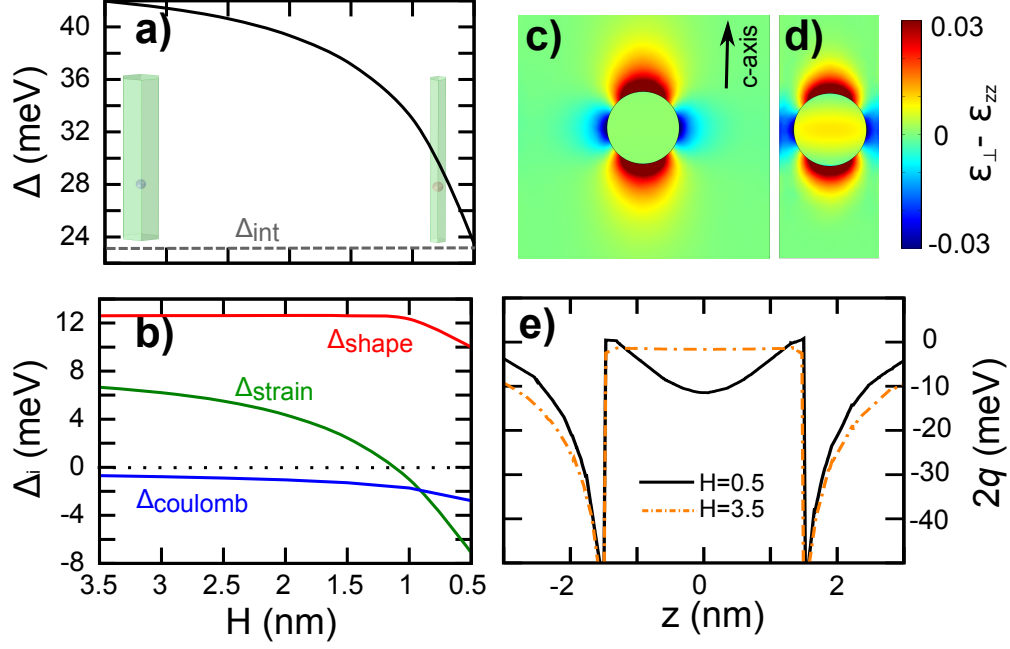


Figure 2: (a) HH-LH splitting as a function of the shell thickness. Dashed lines show the intrinsic splitting  $\Delta_{int}$ , for comparison. (b) Influence of individual factors on  $\Delta$ . Dotted lines highlight the zero. (c) shear strain in and around the core of a thick-shell DiR. (d) same in a thin-shell DiR. Note the finite strain inside the core. (e) Offset between deformation potentials seen by HH and LHs along the rod axis. In the thin shell case ( $H = 0.5$  nm), the difference inside the core becomes negative, thus favoring LHs. In all cases the core is spherical with  $R = 1.5$  nm, and rod length is  $L = 50$  nm.

$H$ , its value being small in all cases. The main change is observed in  $\Delta_{strain}$ , which is positive for thick shells but rapidly decreases as  $H$  gets smaller, reaching negative values for  $H < 1$  nm. This behavior is essentially due to the DP, with PZ playing a secondary role, and can be interpreted as follows. Within the quasi-cubic approximation for wurtzite structures,<sup>20,30</sup> the DP term splitting HH and LH states is (see Supporting Information):

$$2q = 2d/\sqrt{3} (\epsilon_{\perp} - \epsilon_{zz}) \approx \Delta_{strain}, \quad (2)$$

where  $d$  is a cubic deformation potential parameter,  $\epsilon_{\perp} = 1/2(\epsilon_{xx} + \epsilon_{yy})$  and  $\epsilon_{zz}$  strain tensor elements orthogonal and parallel to the  $c$ -axis. The shear term  $(\epsilon_{\perp} - \epsilon_{zz})$  gives the difference between the vertical and in-plane lattice constant due to the strain. Since  $d < 0$  for both CdSe and CdS (see Supporting Information), the splitting decreases for  $(\epsilon_{\perp} - \epsilon_{zz}) > 0$  and increases

otherwise. As shown in Fig.2(c), when the shell is thick, shear strain inside the spherical core is zero. Because the hole wave function is mostly confined inside the core,<sup>28</sup> this means  $\Delta_{strain}$  should be negligible. In Fig.2(b), we observe a small but finite  $\Delta_{strain} \approx 5$  meV, which is due to the wave function leaking into the CdS shell, where shear strain is very pronounced. The relevant change, however, takes place when the shell is made thinner. As shown in Fig.2(d), for small  $H$  values, shear strain becomes positive inside the core. This is because the CdSe core, which is compressed inside the CdS shell, finds it easier to dilate in the thin shell direction. Then,  $|\epsilon_{\perp}|$  becomes smaller than in the thick shell case, while  $|\epsilon_{zz}|$  stays the same. Because both  $\epsilon_{\perp}$  and  $\epsilon_{zz}$  are negative (compressive),  $(\epsilon_{\perp} - \epsilon_{zz}) > 0$ . In other words, strain relaxation in the direction orthogonal to the  $c$ -axis, leads to negative  $\Delta_{strain}$  values stabilizing LH states. This is further illustrated in Fig.2(e), which compares  $2q$  along the  $c$ -axis for thick ( $H = 3.5$  nm) and thin ( $H = 0.5$  nm) shells. When using thin shells, the DP energy offset between HH and LH inside the core decreases by more than 10 meV.

The influence of the shell length  $L$  on  $\Delta$  is much weaker than that of  $H$  (see Fig. S1 in Supporting Information). Its main effect is to stabilize HH with respect to LHs when the shell changes from rod to disk shape (oblate instead of prolate), which actually agrees with previous results for dot-in-plates.<sup>27</sup>

As mentioned above, in spite of the negative  $\Delta_{strain}$  value, the ground state remains HH even for the thinnest shells studied in Fig.2. In order to obtain a LH ground state, one needs to consider the additional effect of the core size and shape, as we show next. We take a fixed, thin shell and vary the core radii  $R_z$  and  $R_{\perp}$ . The resulting  $\Delta$  is shown in Fig.3(a). For spherical cores ( $R_z/R_{\perp} = 1$ ),  $\Delta > 0$  regardless of the core size, but it rapidly decreases with increasing aspect ratio of the core. For  $R_z/R_{\perp}$  between 1.2 and 1.35, depending on the core size,  $\Delta$  becomes negative. This confirms that LH ground states are feasible, but they require slightly prolate cores rather than anisotropic shells.

The fast decrease of  $\Delta$  with the core aspect ratio can be understood from Fig.3(b). As the core becomes more prolate,  $\Delta_{shape}$  decreases because of the anisotropic masses of HH and LH.<sup>23</sup> Yet,

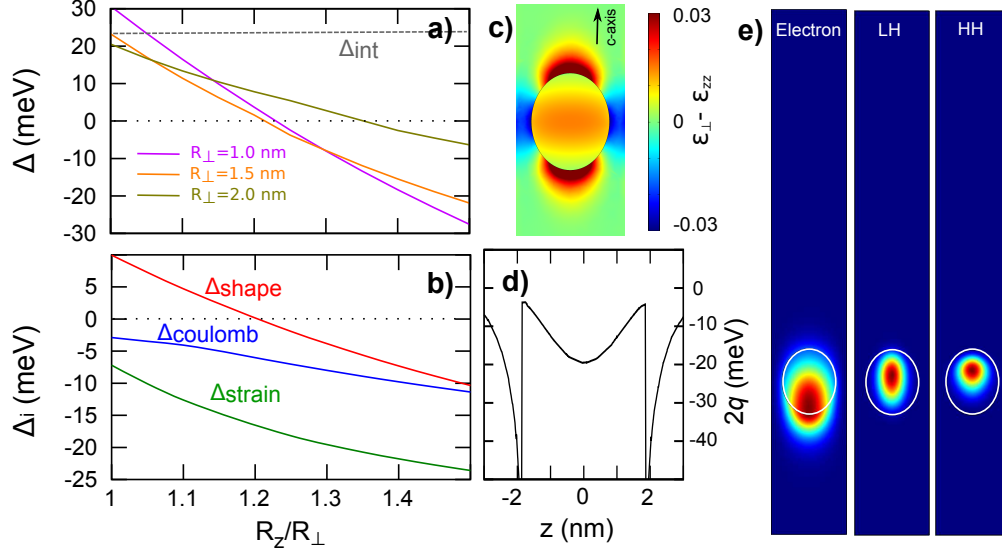


Figure 3: (a) HH-LH splitting as a function of the core aspect ratio for different diameters. (b) Influence of individual factors on  $\Delta$ . Dotted lines highlight the zero. (c) shear strain in and around the core of a prolate-core DiR. (d) Offset between deformation potentials seen by HH and LHs along the rod axis. Notice the value at the center of the core is about twice that of the spherical core in Fig.2(e). (e) Excitonic electron, HH and LH charge densities in a DiR. In all cases the shell has thickness  $H = 0.5$  nm and length  $L = 50$  nm. For panels (b)-(e), the core has  $R_\perp = 1.5$  nm. For panels (c)-(e),  $R_z/R_\perp = 1.25$ .

this term by itself would not suffice to compensate for  $\Delta_{int}$  and obtain a LH ground state. There is an additional negative contribution of  $\Delta_{strain}$ , which is again due to the different DP seen by HHs and LHs. If we compare a spherical core ( $R_z/R_\perp = 1$ , Fig.2(d)) with a slightly prolate one ( $R_z/R_\perp = 1.25$ , Fig.3(c)), it can be seen that the shear strain inside the core is doubled. The same can be observed in the DP offset profile along the rod axis, Fig.3(d), which is twice deeper inside the core as compared to its spherical counterpart (black line in Fig.2(e)). It follows that a small deviation from sphericity has an important effect on  $\Delta_{strain}$ . Fig.3(b) also shows that Coulomb interaction provides a negative contribution to  $\Delta$ , which is enhanced with increasing core aspect ratio. The reason can be inferred from the charge densities plotted in Fig.3(e). The exciton electron and hole charge densities are slightly pushed towards opposite sides of the core along the  $c$ -axis, owing to PZ.<sup>26</sup> Because LHs have lighter mass in this direction, they are more elongated and their overlap with the electron is larger than that of HHs. Consequently, electron-LH Coulomb attraction is stronger than electron-HH one. With increasing core size and ellipticity, this effect

becomes more important and helps stabilize LHs.

Since wurtzite cores tend to grow prolate, all the above effects are expected to contribute in the formation of LH ground states. The critical aspect ratio at which the ground state crossover takes place depends on the core diameter and shell thickness, but we stress small values suffice. In fact, we have checked that using quasi-cubic masses instead of the bulk wurtzite values employed in Fig.3(a), the critical aspect ratio becomes even smaller,  $R_z/R_\perp = 1.15$  or less (see Fig. S2 in Supporting Information). Likewise, using different sets of DP parameters within experimental uncertainty, the critical aspect ratio remains similar or slightly smaller (Fig. S3 in Supporting Information). Please note that the CdS shell plays an important role on the HH-LH reversal. The critical aspect ratio for a CdSe quantum dot is systematically greater than that of a CdSe seed forming a DiR (Fig. S4 in Supporting Information). The fact that large cores are more prone to grow prolate could partly explain the experimental observation that large core DiRs show higher degrees of linear polarization than small ones.<sup>15</sup> On a different note, the seeming contradiction between Ref.<sup>15</sup> and Ref.<sup>19</sup> experiments, which reported LH and HH ground states for DiRs with similar core radius ( $R \approx 3.2$  nm) and shell thickness ( $H \approx 0.5$  nm), respectively, is possibly due to the pronounced prolate shape of the former (see large dots in Fig. 1 of their Supporting Information), as opposed to the quasi-spherical shape claimed by the latter. This would be consistent with our prediction that a thin shell does not suffice to induce a LH ground state, core ellipticity being a requirement.

To see how the HH-LH energy splitting actually affects the degree of linear polarization, we need to include the exciton fine structure induced by electron-hole exchange interaction. We calculate this term with a wurtzite Hamiltonian (see Supporting Information), but the results are in close agreement with the quasi-cubic approximation used in the literature.<sup>31,32</sup> As an example, Fig.4(a) shows the exciton spectrum corresponding to a DiR with small core ( $R_\perp = 1$  nm) and thin shell. In the figure, we use standard exciton notation,  $F^{L/U}$ , where  $F$  is the  $z$ -projection of the total exciton angular momentum and  $L/U$  stands for lower/upper state with a given  $F$ . In the spher-

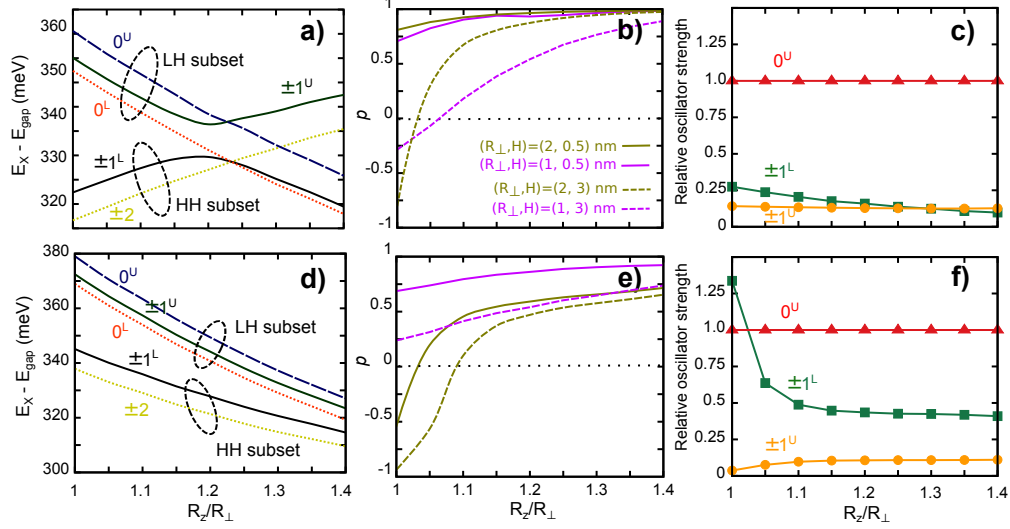


Figure 4: (a) Exciton fine structure dependence on the core aspect ratio for  $R_{\perp} = 1$  nm and  $H = 0.5$  nm. HH and LH subsets cross at an aspect ratio governed by  $\Delta$ .  $0^U$  is the only state emitting linearly polarized light.  $\pm 1^{U/L}$  states emit planar polarized light. Other states (dotted lines) are dark. (b) Degree of linear polarization as a function of the DiR core aspect ratio, for different core sizes and shell thicknesses, at room temperature. Highest  $p$  values correspond to large, prolate cores with thin shells. (c) Oscillator strength of  $\pm 1^{U/L}$  states relative to that of  $0^U$  in DiRs with  $R_{\perp} = 2$  nm and  $H = 0.5$  nm. They are much weaker. (d-f) is the same as (a-c) but neglecting strain. In all the plots the shell has aspect ratio of 10, so that dielectric effects are constant.

ical core limit,  $R_z/R_{\perp} = 1$ , there are two subsets of exciton levels. The lower subset is formed by  $\pm 2$  and  $\pm 1$  doublets.  $\pm 2$  are optically inactive states, while  $\pm 1^L$  emit planar polarized light orthogonal to the  $c$ -axis. All these states are essentially HH in nature. The upper subset of exciton levels is formed by LH states instead.  $0^L$  is optically inactive,  $\pm 1^U$  emits planar polarized light and  $0^U$  emits exclusively linearly ( $z$ -)polarized light, because spin selection rules only allow the  $C$ -band component of the LH to recombine with the electron.<sup>31</sup> The energy splitting between HH and LH subsets is roughly given by  $\Delta$ . Thus, HH and LH subsets cross at  $R_z/R_{\perp} \approx 1.2$ , similar to Fig.3(a). Qualitatively similar fine structure spectra are obtained for larger cores, but with smaller intra-subset splittings due to the weaker Coulomb interaction (not shown).

Notice in Fig.4(a) that  $0^U$  is never the ground state. Even for  $R_z/R_{\perp} > 1.2$ , when  $\Delta < 0$ ,  $\pm 1^L$  states are lower in energy, and they emit planar polarized light. Thus, a net linearly polarized exciton emission requires thermal energy. Negative  $\Delta$  values help increase the thermal occupation of  $0^U$ , but a for a complete understanding of room temperature polarization one has to compare

and analyze the emission from several competing states. We then calculate the polarization degree:

$$p = \frac{I_z - I_{\perp}}{I_z + I_{\perp}}, \quad (3)$$

where  $I_z$  is the intensity of light emitted along the  $c$ -axis, given by:

$$I_z = N_{0U} R_z^e f_{0U} \quad (4)$$

and  $I_{\perp}$  that in an arbitrary direction perpendicular to it:

$$I_{\perp} = 2 \times R_{\perp}^e (N_{\pm 1L} f_{\pm 1L} + N_{\pm 1U} f_{\pm 1U}). \quad (5)$$

In the above expressions,  $N_{F^{U/L}}$  is the room temperature occupation of the state  $F^{U/L}$ ,  $f_{F^{U/L}}$  the corresponding oscillator strength, and  $R_z^e$  ( $R_{\perp}^e$ ) the local field parameter, accounting for the dielectric screening of electromagnetic fields along the  $c$ -axis (orthogonal to it). Since the last term depends on the aspect ratio of the shell only, we choose DiRs with fixed aspect ratio of 10, so that all differences we may observe arise solely from electronic factors. The factor 2 in Eq. (5) accounts for the state degeneracy.

Fig.4(b) shows the calculated degree of polarization for DiRs with different geometries. Important differences are observed, which shows that  $p$  is not governed by the shell aspect ratio alone, as sometimes suggested.<sup>5</sup> Given a fixed core size, linear polarization is much more pronounced for thin CdS shell (solid lines) than for thick shell (dashed lines), in agreement with the experiments of Refs.<sup>15,18</sup> Besides, core ellipticity is found to have a major influence. The highest degrees of linear polarization are obtained for prolate core no matter the shell thickness. This is consistent with experiments showing that rod-in-rods have  $p$  values systematically larger than DiRs.<sup>16,17</sup> Both these effects can be understood from the geometry-induced decrease of  $\Delta$ , which translates into larger  $N_{0U}$ . Note however that strong polarization  $p$  can be achieved even if  $\Delta > 0$ . For example, a spherical core with  $(R_{\perp}, H) = (1.0, 0.5)$  nm has  $p = 0.71$  in spite of having  $\Delta = 30$  meV. This shows that

even for relatively low  $N_{0U}$ , dielectric effects and the relative oscillator strengths  $f_{F^{U/L}}$  can lead to net linear polarization.

On the other hand, Fig.4(b) also shows that larger cores generally show higher  $p$  values than small ones. This is in close agreement with the central experimental observation of Ref.,<sup>15</sup> namely that the core size is a chief factor determining  $p$  in DiRs, but again it is beyond purely energetic interpretations, since –as shown on Fig.3(a)– large cores require higher core aspect ratio for LHs to become ground state. The interpretation of this phenomenon is as follows. In large cores, the oscillator strength  $f_{0U}$  is much larger than that of other thermally populated states emitting  $(x,y)$ -polarized light. This is illustrated in Fig. Fig.4(c) for DiRs with  $(R_{\perp}, H) = (2, 0.5)$  nm: if the core is spherical,  $f_{0U}$  is 4-6 times larger than  $f_{\pm 1L}$  and  $f_{\pm 1U}$ , and the difference increases as the core becomes prolate. The underlying reason can be seen in Fig.3(e): shear strain-induced PZ in large core DiRs leads to stronger (weaker) electron-LH (HH) overlap, thus stimulating emission from  $0^U$  (LH) relative to  $\pm 1^U$  (HH). In general, this effect scales with core size and ellipticity (see Figs. S5 and S6 in the Supporting Information). The faster recombination of LH excitons implies that pronounced linear polarization can be achieved even if the ground state is HH.

To further evidence the critical role of strain DP and PZ in determining the optical anisotropy of DiRs, in Fig.4(d-f) we show the fine structure spectrum, degree of linear polarization and relative oscillator strengths obtained neglecting core/shell strain. One can see that the ground state remains HH,  $f_{\pm 1L}$  is closer to  $f_{0U}$  and, consequently, the polarization value  $p$  is much smaller than in the strained case. In fact, small radii now imply stronger linear polarization, in sharp contradiction with Ref.<sup>15</sup> experiments. It follows strain is crucial.<sup>33</sup>

In summary, we have shown theoretically that linearly polarized light emission and absorption in core/shell CdSe/CdS DiRs has an electronic origin associated with (i) the energetic stabilization of LHs with respect to HHs, and (ii) the enhanced recombination rate of LH excitons compared to HH ones. The energetic stabilization of LHs takes place upon the growth of the CdS shell around the CdSe seed, mainly via shear strain, with additional contributions from electron-hole Coulomb interaction and quantum confinement. Shear strain,  $\epsilon_{\perp} - \epsilon_{zz}$ , is roughly zero inside

spherical CdSe cores, but wurtzite cores tend to grow slightly prolate along the  $c$ -axis. In such a case,  $\epsilon_{zz}$  becomes more compressive and  $(\epsilon_{\perp} - \epsilon_{zz}) > 0$ , which stabilizes LHs relative to HHs via deformation potential. A thin diameter CdS shell has a similar –albeit weaker– influence on shear strain, as it enables the core to dilate in the transversal direction and hence relax  $\epsilon_{\perp}$ . The enhanced recombination rate of LH excitons is in turn related to shear strain-induced PZ, which becomes important in DiRs with large, prolate core.<sup>26</sup> Piezoelectric fields push electron and hole wave functions towards opposite sides of the core. This effect is more pronounced for HHs than for LHs, owing to their heavier masses along the  $c$ -axis. Consequently,  $0^U$  states have faster radiative recombination rates than  $\pm 1^L$  and  $\pm 1^U$ , and room temperature emission becomes linearly polarized.

From our analysis, it follows that the geometrical conditions optimizing linear polarization in DiRs are prolate core shape (enhanced shear strain, large PZ dipole and electron-LH attraction), large core size (large PZ dipole, weak confinement), and thin shell (enhanced shear strain). These findings support and provide a unified explanation for recent experimental works, which phenomenologically inferred similar geometric conditions.<sup>15–18</sup> Together with the well-known dielectric origin of linear polarization in rod-shaped structures,<sup>12</sup> our results complete the theoretical knowledge required for deterministic engineering of absorption and emission anisotropy in DiRs.

## Acknowledgement

Support from MINECO project CTQ2014-60178-P, UJI project P1-1B2014-24 is acknowledged.

**Supporting Information Available:** Methods, material parameters, additional calculations on: the effect of the rod length; robustness against the use of different sets of masses and deformation potential parameters; CdSe seeds with no shell; dependence of e-LH/HH overlap vs core size in DiRs.

## References

- (1) Kovalenko M.; Manna L.; Cabot A.; Hens Z.; Talapin D.V.; Kagan Ch.R.; Klimov V.I.; Rogach A.L.; Reiss P.; Milliron D.J.; *et al.* Prospects of Nanoscience with Nanocrystals. *ACS Nano* **2015**, *9*, 1012-1057.
- (2) Sitt A.; Hadar I.; Banin U. Band-Gap Engineering, Optoelectronic Properties and Applications of Colloidal Heterostructured Semiconductor Nanorods. *Nano Today* **2013**, *8*, 494-513.
- (3) Talapin D.V.; Koeppel R.; Gotzinger S.; Kornowski A.; Lupton J.M.; Rogach A.L.; Benson O.; Feldmann J.; and Weller H. Highly Emissive Colloidal CdSe/CdS Heterostructures of Mixed Dimensionality. *Nano Lett* **2003**, *3*, 1677-1681.
- (4) Carbone L.; Nobile C.; De Giorgi M.; Della Sala F.; Morello G.; Pompa P.; Hytch M.; Snoeck E.; Fiore A.; Franchini I.R.; *et al.* Synthesis and Micrometer-Scale Assembly of Colloidal CdSe/CdS Nanorods Prepared by a Seeded Growth Approach. *Nano Lett* **2007**, *7*, 2942-2950.
- (5) Coropceanu I.; Rossinelli A.; Caram J.R.; Freyria F.S.; Bawendi M.G. Slow-Injection Growth of Seeded CdSe/CdS Nanorods with Unity Fluorescence Quantum Yield and Complete Shell to Core Energy Transfer. *ACS Nano* **2016**, *10*, 3295-3301.
- (6) Müller J.; Lupton J.M.; Rogach A.L.; Feldmann J.; Talapin D.V.; Weller H. Monitoring Surface Charge Movement in Single Elongated Semiconductor Nanocrystals. *Phys. Rev. Lett.* **2004**, *93*, 167402.
- (7) Saba M.; Minniberger S.; Quochi F.; Roither J.; Marceddu M.; Gocalinska A.; Kovalenko M.V.; Talapin D.V.; Heiss W.; Mura A.; Bongiovanni G. Exciton-exciton Interaction and Optical Gain in Colloidal CdSe/CdS Dot/Rod Nanocrystals. *Adv. Mater* **2009**, *21*, 4942-4946.
- (8) Di Stasio F.; Grim J.Q.; Lesnyak V.; Rastogi P.; Manna L.; Moreels I.; Krahn R. Single-

- Mode Lasing from Colloidal Water-Soluble CdSe/CdS Quantum Dot-in-Rods. *Small* **2014**, *11*, 1328-1334.
- (9) Raino G.; Stoferle T.; Moreels I.; Gomes R.; Kamal J.S.; Hens Z.; Mahrt R.F. Probing the Wave Function Delocalization in CdSe/CdS Dot-in-Rod Nanocrystals by Time- and Temperature-Resolved Spectroscopy. *ACS Nano* **2011**, *5*, 4031-4036.
- (10) Allione M.; Ballester A.; Li H.; Comin A.; Movilla J.L.; Climente J.I.; Manna L.; Moreels I. Two-Photon-Induced Blue Shift of Core and Shell Optical Transitions in Colloidal CdSe/CdS Quasi-Type II Quantum Rods. *ACS Nano* **2013**, *7*, 2443-2452.
- (11) Chen Y.; Vela J.; Htoon H.; Casson J.L.; Werder D.J.; Bussian D.A.; Klimov V.I.; Hollingsworth J.A. "Giant" Multishell CdSe Nanocrystal Quantum Dots with Suppressed Blinking. *J. Am. Chem. Soc.* **2008**, *130*, 5026-5027.
- (12) Shabaev A.; Efros A.L. 1D Exciton Spectroscopy of Semiconductor Nanorods. *Nano Lett.* **2004**, *4*, 1821-1825.
- (13) Kamal J.S.; Gomes R.; Hens Z.; Karvar M.; Neyts K.; Compernelle S.; Vanhaecke F. Direct Determination of Absorption Anisotropy in Colloidal Quantum Rods. *Phys. Rev. B* **85**, 035126 (2012).
- (14) Hu J.; Li L.S.; Yang W.; Manna L.; Wang L.W.; Alivisatos A.P. Linearly Polarized Emission from Colloidal Semiconductor Quantum Rods. *Science* **2001**, *292*, 2060-2063.
- (15) Vezzoli S.; Manceau M.; Leménager G.; Glorieux Q.; Giacobino E.; Carbone L.; De Vittorio M.; Bramati A. Exciton Fine Structure of CdSe/CdS Nanocrystals Determined by Polarization Microscopy at Room Temperature. *ACS Nano* **2015**, *8*, 7992-8003.
- (16) Sitt A.; Salant A.; Menagen G.; Banin U. Highly Emissive Nano Rod-in-Rod Heterostructures with Strong Linear Polarization. *Nano Lett* **2011**, *11*, 2054-2060.

- (17) Hadar I.; Hitin G.B.; Sitt A.; Faust A.; Banin U. Polarization Properties of Semiconductor Nanorod Heterostructures: From Single Particles to the Ensemble. *J. Phys. Chem. Lett.* **2013**, *4*, 502-507.
- (18) Diroll B.T.; Koschitzky A.; Murray C.B. Tunable Optical Anisotropy of Seeded CdSe/CdS Nanorods. *J. Phys. Chem. Lett.* **2014**, *5*, 85-91.
- (19) Granados del Águila A.; Jha B.; Pietra F.; Groeneveld E.; de Mello Donegá C.; Maan J.; Vanmaekelbergh D.; Christianen P.C.M. Observation of the Full Exciton and Phonon Fine Structure in CdSe/CdS Dot-in-Rod Heteronanocrystals. *ACS Nano* **2014**, *6*, 5921-5931.
- (20) Chuang S.L.; Chang C.S. k-p Method for Strained Wurtzite Semiconductors. *Phys. Rev. B* **1996**, *54*, 2491-2503.
- (21) Climente J.I.; Segarra C.; Rajadell F.; Planelles J. Electrons, Holes, and Excitons in GaAs Polytype Quantum Dots. *J. Appl. Phys.* **2016**, *119*, 125705.
- (22) Li L.S.; Alivisatos A.P. Origin and Scaling of the Permanent Dipole Moment in CdSe Nanorods. *Phys. Rev. Lett.* **2003**, *90*, 097402.
- (23) Efros A.L.; Rodina A.V. Band-edge Absorption and Luminescence of Nonspherical Nanometer-Size Crystals. *Phys. Rev. B* **1993**, *47* 10005.
- (24) Planelles J.; Rajadell F.; Climente J.I. Hole Band Mixing in CdS and CdSe Quantum Dots and Quantum Rods. *J. Phys. Chem. C* **2010**, *114*, 8337-8342.
- (25) Christodoulou S.; Rajadell F.; Casu A.; Vaccaro G.; Grim J.; Genovese A.; Manna L.; Climente J.I.; Meinardi F.; Raino G.; *et al.* Band Structure Engineering via Piezoelectric Fields in Strained Anisotropic CdSe/CdS Nanocrystals. *Nat. Commun.* **2015**, *6*, 7905.
- (26) Segarra C.; Climente J.I.; Polovitsyn A.; Rajadell F.; Moreels I.; Planelles J. Piezoelectric Control of the Exciton Wave Function in Colloidal CdSe/CdS Nanocrystals. *J. Phys. Chem. Lett.* **2016**, *7*, 2182-2188.

- (27) Cassette E.; Mahler B.; Guigner J.M.; Patriarche G.; Dubertret B.; Pons T. Colloidal CdSe/CdS Dot-in-Plate Nanocrystals with 2D-Polarized Emission. *ACS Nano* **2012**, *6*, 6741-6750.
- (28) Luo Y.; Wang L.W. Electronic Structures of the CdSe/CdS Core-Shell Nanorods. *ACS Nano* **2010**, *4*, 91-98.
- (29) Eshet H.; Grünwald M.; Rabani E. The Electronic Structure of CdSe/CdS Core/Shell Seeded Nanorods: Type-I or Quasi-Type-II? *Nano Lett.* **2013**, *13*, 5880-5885.
- (30) Xia J.B.; Li J. Electronic Structure of Quantum Spheres with Wurtzite Structure. *Phys. Rev. B* **1999**, *60*, 11540-11544.
- (31) Efros Al.L.; Rosen M.; Kuno M.; Nirmal M.; Norris D.J.; Bawendi M. Band-Edge Exciton in Quantum Dots of Semiconductors with a Degenerate Valence Band: Dark and Bright Exciton States. *Phys. Rev. B* **1996**, *54*, 4843-4856.
- (32) Raino G.; Stoferle T.; Moreels I.; Gomes R.; Hens Z.; Mahrt R. Controlling the Exciton Fine Structure Splitting in CdSe/CdS Dot-in-Rod Nanojunctions. *ACS Nano* **2012**, *6*, 1979-1987.
- (33) A comparison between Fig.4(c) and (f) shows that unstrained oscillator strengths like those of Ref.<sup>31</sup> are unsuited for analysis of DiRs. Thus, the quantitative data fitting of Ref.<sup>15</sup> should be taken with care.